APPLICATION OF ADAPTIVE WALLS IN CASCADE WIND TUNNELS

H.-J. Rehder

Institute for Experimental Fluid Mechanics, DLR
Bunsenstrasse, 10, 3400 Göttingen, Germany

Summary

To improve the periodicity and to reduce the number of blades in test sections of rectilinear cascade wind tunnels flexible adaptive upper and lower walls are very useful. The adaptive walls must be shaped to contours through a cascade flow field of infinite length.

In the present paper a computational adaptation method is described which determines the required wall deflections from pressure distributions measured along the flexible walls. This scheme is applicable for cascades with incompressible flows and for low deflection cascades with compressible subsonic flows. The process can change the inlet flow angle of the cascade to a desired value.

The verification of the adaptation scheme is shown for some theoretical examples. Finally the design of a new adaptive wall test section in the wind tunnel for rectilinear cascades (EGG) of the DLR Göttingen is presented.

Nomenclature

E_1, E_2	influence functions, Eqs. (6) and (7)
h	channel high
ℓ	chord length
n_p	number of blades in the test section
M_0	strength of a doublet
R	radius
s_o, s_u	coordinates along the adaptive walls
t	pitch length
$W = U - iV$	complex velocity vector
$w = u - iv$	complex disturbance velocity vector
$z = x + iy$	complex coordinate in the flow field
ß	flow angle (measured from circumferential direction)
$ß_s$	stagger angle
Γ_0	strength of a vortex
$\zeta = \xi + i\eta$	complex coordinate on the integration path
λ	stagger angle of a row of vortices or doublets

Subscripts

∞	free stream condition
1	homogeneous inlet flow
2	homogeneous outlet flow
c	integration path
Cas	due to the cascade
Wi	due to the wall interference
ν	number of the integration path, Eq. (2)

1. Introduction

Experimental investigations on rectilinear cascades are of great importance for the design of axial turbomachines. A rectilinear cascade is defined by unrolling a stream surface of revolution through the blade ring of a stator or rotor, see **Fig. 1**. The highly three-dimensional flow in a turbomachine is then reduced to a two-dimensional flow field through a cascade of infinite length.

For experimental studies only a part of an infinite cascade flow field can be tested in a wind tunnel. So the upper and lower test section walls form the boundaries of the cascade in the circumferential direction. These walls are directly responsible for the conditions of the flow field. Basically, there are two possibilities for reaching a good flow condition (periodicity) in a cascade test section:

- In general, as in the wind tunnel for rectilinear cascades (EGG) of the DLR [1], only straight upper and lower walls upstream and free shear layers downstream of the cascade represent the boundaries of the flow field. By mounting a sufficiently large number of blades inside the test section (up to 15 profiles) a nearly good periodicity in the middle of the cascade flow field is obtained.
- A new and not as yet applied possibility of simulating a part of an infinite cascade flow field is to build a test section with upper and lower adaptive walls. These walls can be made of flexible steel plates which are deformed by a set of motor driven jacks to any desired contour. With such an arrangement a very good periodicity in a cascade test section is achieved and this allows the reduction of the number of blades to at least just one blade (one passage).

A new cascade test section with adaptive walls for the EGG was designed in the DLR Institute of Experimental Fluid Mechanics in Göttingen [2]. In conjuction with such adaptive or "self streamlining" wind tunnels computer codes for the calculation of the adapted wall contours are very important. In the past such codes were developed for the application in conventional wind tunnels with two-dimensional adaptive test sections, see for instance [3]. Now a new computational code for adaptive cascade test sections and its verification is presented in the first part of this paper [4]. The last part gives a description of the adaptive walled EGG test section.

2. A wall adaptation scheme for cascade test sections

The principle of a wall adaptation scheme as described in [3] requires the measurement of two independent flow variables at the adaptive walls, for example the tangential and normal velocity components. An equivalent pair of variables are the wall pressure and the wall contour from which the velocity components can be determined. These flow variables are measured in an initial wind tunnel run and used as input for the calculation of the adapted wall contours. Normally this adaptation is done iteratively with a new tunnel run with measured flow variables along the walls and new calculated wall contours in every step. The iteration stops until the differences between the wall contours before and after a step (wall displacements) are zero and thus complete adaptation is obtained.

The wall adaptation method for cascade test sections which is described below is based on a scheme as shown in [3]. But there is one difference for the application of both methods. In a conventional adaptive test section (for example with an airfoil) the adaptation [3] is done to a flow field which passes into undisturbed parallel flow at infinity. In contrast to that the adaptation in a cascade test section must be done to a periodic cascade flow field of infinite length [4,5].

2.1 General description

The starting point is a cascade test section with adaptive upper and lower walls and any desired number of blades inside, see **Fig. 2**. It is accepted that the walls are not adapted. The test section itself will now be continued along the cascade direction (y-axis). This results in a configuration of a cascade of infinite length with a periodic arrangement of the adaptive contours in the distance $n_p \cdot t$. The upper and lower walls are able to represent different contours in a blade channel if there is a definite area between them [4]. But it is also possible for both walls to form identical streamlines. Then the area between the walls is reduced to zero (Fig. 2).

The flow field in Fig. 2 must be described by the potential theory [5] and is a superposition of the cascade flow field, induced by singularities on the blade contours, with the interference flow field of all adaptive walls, induced by singularities on the walls or in the definite areas between the walls.

The wall interferences inside the whole cascade test section will now be calculated by the Cauchy integral formula [4,6]:

$$w_{Wi}(z) = \sum_{\nu=-\infty}^{+\infty} \frac{1}{2 \cdot \pi \cdot i} \oint_{C_\nu} \frac{w_c(\zeta_\nu)}{\zeta_\nu - z} \cdot d\zeta_\nu \tag{1}$$

The integration paths C_ν with the complex coordinates ζ_ν enclose the adaptive contours in Fig. 2. w_c is the known complex disturbance velocity vector along these paths. The components u_c and v_c of this vector can be determined from wall pressure distribution measurements which are obtained from an initial wind tunnel run. In the far field upstream and downstream of the cascade constant flow conditions will occur, and so the disturbance velocity w_c along the parts of the integration paths which cut the walls can be assumed as constant. Having the advantage that only singularities inside the integration paths (on and between the adaptive walls) have an influence in the Cauchy integral [4,6] only the complex disturbance velocity vector w_{Wi} induced by the walls is obtained on the left side in Eq. (1). z is the complex coordinate in the test section where these wall interferences have to be calculated.

With the equation

$$\zeta_\nu = \zeta_0 + i \cdot \nu \cdot n_p \cdot t \quad (\nu = 0, \pm 1, \pm 2, \ldots \pm \infty) \tag{2}$$

all points of the integration paths C_ν are described on a straight line parallel to the cascade direction (Fig. 2). Inserting Eq. (2) into Eq. (1) gives after some transformations:

$$w_{Wi}(z) = \frac{i}{2 \cdot n_p \cdot t} \oint_C w_c(\zeta) \cdot \coth\left[\frac{(z-\zeta)\pi}{n_p \cdot t}\right] \cdot d\zeta \tag{3}$$

This is the base equation for the calculation of wall interferences inside a cascade test section. The integration (in clockwise direction) has to be carried out only along the integration path $\nu = 0$. After separating the real and imaginary parts of Eq. (3) we obtain:

$$u_{Wi} = +\frac{1}{2 \cdot n_p \cdot t}\left[\oint_C (E_1 \cdot u_c + E_2 \cdot v_c) \cdot d\xi - \oint_C (E_2 \cdot u_c - E_1 \cdot v_c) \cdot d\eta\right], \tag{4}$$

$$v_{Wi} = -\frac{1}{2 \cdot n_p \cdot t}\left[\oint_C (E_2 \cdot u_c - E_1 \cdot v_c) \cdot d\xi + \oint_C (E_1 \cdot u_c + E_2 \cdot v_c) \cdot d\eta\right]. \tag{5}$$

The functions E_1 and E_2 can be calculated from:

$$E_1 = \frac{\sin(2\pi \frac{y-\eta}{n_p \cdot t})}{\cosh(2\pi \frac{x-\xi}{n_p \cdot t}) - \cos(2\pi \frac{y-\eta}{n_p \cdot t})}, \tag{6}$$

$$E_2 = \frac{\sinh(2\pi \frac{x-\xi}{n_p \cdot t})}{\cosh(2\pi \frac{x-\xi}{n_p \cdot t}) - \cos(2\pi \frac{y-\eta}{n_p \cdot t})}. \tag{7}$$

Eq. (4) and Eq. (5) give the components u_{Wi} and v_{Wi} of the wall induced velocity vector w_{Wi} in the whole cascade test section from the known disturbance velocities u_c and v_c along the adaptive walls, see Fig. 2.

Now the flow field in the test section is assumed to be a linear superposition of the cascade flow with the interference flow of the adaptive walls:

$$u = u_{Cas} + u_{Wi}, \tag{8}$$

$$v = v_{Cas} + v_{Wi}. \tag{9}$$

Near the walls the velocities are known from measured pressure distributions ($u = u_c$, $v = v_c$). After calculating there the wall interferences u_{Wi} and v_{Wi} from the Eqs. (4) and (5) the interference free disturbance velocities u_{Cas} and v_{Cas} of the cascade are obtained from Eq. (8) and Eq. (9). With these interference free velocities streamlines can be integrated along the upper and lower walls which give the adapted wall contours [4].

With these new contours a reset iteration step, i.e. a new tunnel run with measured wall pressures and a new calculation of the adapted contours from the Eqs. (4) to (9) can be started. But it is shown in [3] and [4], that with the assumption of a linearized potential flow field and only small wall displacements (between the not adapted and the adapted contours), the adaptation can be achieved within one step. Then after the first step the cascade flow field in the test section is wall interference free and the wall induced velocities u_{Wi} and v_{Wi} which are calculated from the Eqs. (4) and (5) in a second iteration step must be zero.

It should be mentioned that with the assumption of a potential flow field the adaptive walls as shown here (Fig. 2) are only the boundaries of the inviscid flow. The deviation of these contours from the "physical" adaptive walls is the displacement thickness of the boundary layer which can be determined from known pressure distributions on the walls. So in every adaptation step with new measured pressure distrib-

utions the adaptive contours must be corrected by the displacement thickness of the boundary layer.

The above adaptation method is demonstrated for incompressible flow fields. By applying the Prandtl-Glauert equation for rectilinear cascades [5] an expansion to compressible subsonic flow fields is possible. But then the scheme is restricted only to cascades with low deflections and thin profiles (small flow disturbances).

2.2 Test results

The validity of the wall adaptation method will now be tested on some theoretical examples. These are simple cascade flow fields obtained by superimposing the disturbance velocities of vortex or doublet rows with a uniform free stream flow field.

At first the flow field of a vortex in a straight channel is calculated from an alternating infinite row of vortices [4], see **Fig. 3**. The straight streamlines of this flow field are then the upper and lower channel walls. By superimposing this configuration with the flow field of an infinite doublet row [4] with the same spacing h, see **Fig. 4**, we will obtain the flow field of a rotating cylinder inside a straight channel. The calculated disturbance velocities on the walls are then the measured input values for the wall adaptation scheme.

In the first example in **Fig. 5** the adaptation is done to an unstaggered row of rotating cylinders. The upper diagrams show the disturbance velocities along the test section walls. The dashed lines represent the "measured" input values, i.e. the disturbance velocities u_c and v_c along the upper and lower not adapted contours (straight channel walls). The solid curves were obtained after the adaptation process with the Eqs. (4) to (9) and are the interference free disturbance velocities u_{Cas} and v_{Cas} of the rotating cylinder cascade. From these velocities the wall deflections have been calculated which are plotted in the last diagram in Fig. 5. The streamline integration for these adapted countours is started from the cascade front ($s_o = 0$, $s_u = 0$) upstream and downstream into the flow field [4]. Because of the test section high h which is equal to the pitch t of the cascade both adaptive walls represent identical streamlines. In the far field upstream and downstream of the cascade the interference free velocities are constant ($u_{Cas} = 0$, $v_{Cas} = \text{const.}$) and a schematic velocity triangle can be drawn (Fig. 5) which is a typical triangle for an impulse cascade [5].

Fig. 6 shows the adaptation to a 30 degree staggered row of rotating cylinders. The adaptation scheme needs a coordinate system parallel and perpendicular to the cascade direction (see Fig. 2) which deviates from the coordinate system in Fig. 6. So before and after the adaptation the velocities and wall contours must be transformed back and forth between these two coordinate systems. The interference free velocity vector w_{Cas} in the far field now has a component $u_{Cas} = w_{Cas} \cdot \sin \lambda$ in the x-direction and a component $v_{Cas} = w_{Cas} \cdot \cos \lambda$ in the y-direction. This leads to a schematic velocity triangle for a deceleration or compressor cascade [5]. By inclining the cascade front with a negative angle λ, a velocity triangle and a simple flow field through an acceleration or turbine cascade [5] will also be obtained.

In the previous examples the free stream velocity vector W_∞ was set parallel to the x-direction. But it is necessary to investigate a cascade under a desired inlet flow velocity vector W_1 for which the correct direction and value of W_∞ have to be found.

This process is shown schematically in **Fig. 7**. At first W_∞ is set in the desired inlet flow direction. Then the wall interferences and the cascade velocities will be determined with the equations in section 2.1 only for one point on the adaptive walls in the upstream far field of the cascade (Fig. 2). From that we will obtain a velocity triangle drawn with the solid lines in Fig. 7. Now the free stream vector W_∞ is corrected to $W_{\infty N}$ so that the inlet flow vector W_1 could be expected in the desired direction. The measured disturbance velocities u_c and v_c along the adaptive walls must be referred to as $W_{\infty N}$. Now a new calculation of the wall interferences and the cascade velocities for the same point in the upstream far field gives a velocity triangle with the dashed lines in Fig. 7 in which the inlet flow vector W_{1N} deviates again from the desired direction. This is due to the effect that the blade circulation Γ_B and so the cascade velocity w_y changes with the free stream vector W_∞ [5]. Finally this leads to an iterative scheme with a new change of W_∞ in every step. After having found the right free stream vector W_∞ for a desired inlet flow the complete adaptation method as shown in section 2.1 could be performed.

In **Fig. 8** the inlet flow vector W_1 for a staggered cascade of rotating cylinders is set parallel to the x-direction. But now the circulation Γ_0 of the cylinders does not change with the free stream vector W_∞ and so the above described iteration process has ended after the first step. The disturbance velocities in Fig. 8 are now referred to the inlet flow vector W_1 and with a streamline integration started from the upstream far field we will achieve a wall deflection as shown in the last diagram.

3. Design of an adaptive walled cascade test section

Fig. 9 shows a sketch of a new adaptive walled test section for the wind tunnel for rectilinear cascades (EGG) of the DLR. The design of this test section has been planned since 1984. The EGG is an intermittent vacuum type tunnel running with atmospheric air. A more detailed description of this facility is given in reference [1].

The whole adaptive test section for the EGG will be enclosed in a plenum chamber, see Fig. 9. The test section's width (blade high) is 125*mm*. The most important details are the flexible adaptive top and bottom walls, made of 2*mm* thick steel plates, which can be set to desired contours by up to 32 jacks. The jacks are spindle gears driven by stepper motors. To match the adaptive contours to various types of cascades with different inlet angles, the flexible walls and associated jacks are mounted to supports which are adjustable in horizontal and vertical directions. These supports and the rotating disks (which support the actual cascade) will be driven by stepper motors too. The adaptive walls in the cascade region and downstream of the cascade are only incompletely drawn in Fig. 9. These parts of the walls must be exchangeable for different cascades with various downstream flow fields and exit flow angles. Pressure taps along the center line of all adaptive walls enable pressure distribution measurements which can be used as input for wall adaptation methods. More details of this new test section are reported in reference [2].

There are two main reasons to build such a new cascade test section with adaptive walls. The first one is to improve the flow quality over all the flow passages. Second, the side wall boundary layers will be minimized by reducing the distance between the horizontal contraction of the inlet nozzle and the cascade.

Ready designed and manufactured are only the flexible adaptive walls, and the associated jacks and movable supports (Fig. 9). The upper wall is already mounted onto a test rack and its electrical instrumentation is completed. This enables the testing of the jack mechanisms and the stepper motor control systems. A microcomputer PDP 11/73 is available for the control of the wall adjustment process.

4. Conclusions

The wall adaptation method and the design of a new adaptive walled cascade test section as shown here are the first steps in the work about "self streamlining" wind tunnels for rectilinear cascades which is done in the DLR Institute of Experimental Fluid Mechanics. To go on with this work and to improve the experience in adaptive walls for cascades further activities are planned for the future:

- To build a simple low speed adaptive cascade test section with one great blade: The flexible walls and associated jacks and supports designed and manufactured for the new EGG test section (see section 3) will be used for this test section. Investigations on this facility will be started in the near future.
- To develop an adaptation scheme for compressible subsonic cascade flows with high deflections and one for transonic cascade flow: It may be possible to expand the scheme which is presented here to subsonic high deflected cascades, but the application is not correct if supersonic parts of the flow field (with shocks) reach the adaptive test section walls. So in the transonic case other adaptation methods have to be found.

5. References

[1] Heinemann, H.-J.: *The Test Facility for Rectilinear Cascades (EGG) of the DFVLR.* DFVLR-AVA-IB 222-83 A 14 (1983).

[2] Rehder, H.-J.: *Entwurf einer adaptiven Meßstrecke am Windkanal für ebene Gitter (EGG) der DLR.* DLR-IB 222-90 A 01 (1990).

[3] Amecke, J.: *Direkte Berechnung von Wandinterferenzen und Wandadaption bei 2-dimensionaler Strömung in Windkanälen mit geschlossenen Wänden.* DFVLR-FB 85-62 (1985).

[4] Rehder, H.-J.: *Ein Verfahren zur Berechnung der Wandinterferenzen und Wandadaption in Windkanälen für ebene Schaufelgitter (Theoretische Grundlagen).* DLR-IB 222-90 A 30 (1990).

[5] Scholz, N.: *Aerodynamik der Schaufelgitter.* Band I: Grundlagen, 2-dimensionale Theorie, Anwendungen. Karlsruhe: G. Braun 1965.

[6] Hurwitz, A., Courant, R.: *Allgemeine Funktionentheorie und elliptische Funktionen.* Berlin, Göttingen, Heidelberg, New York: Springer 1964.

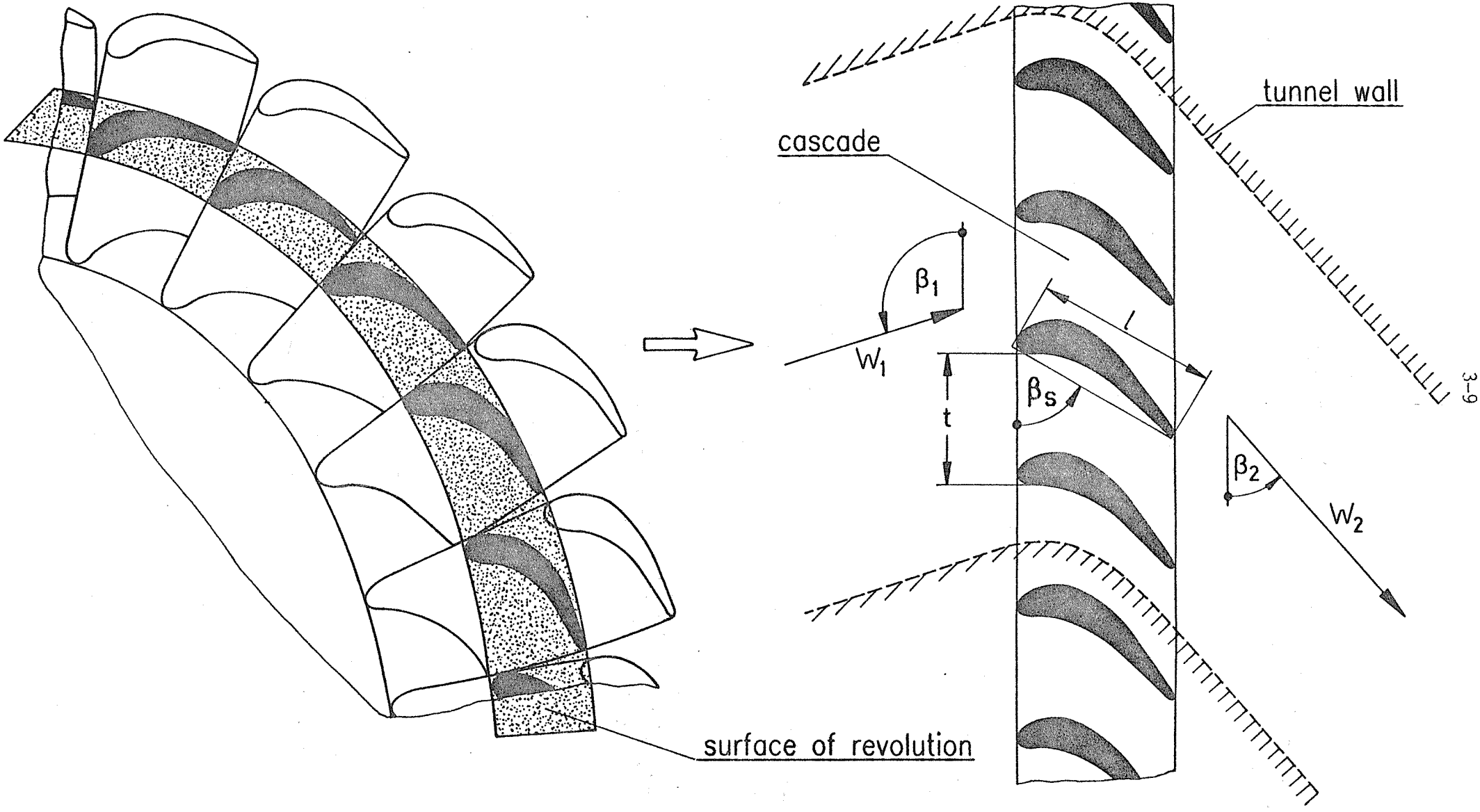

Fig. 1: Reduction from a turbine rotor to a rectilinear cascade

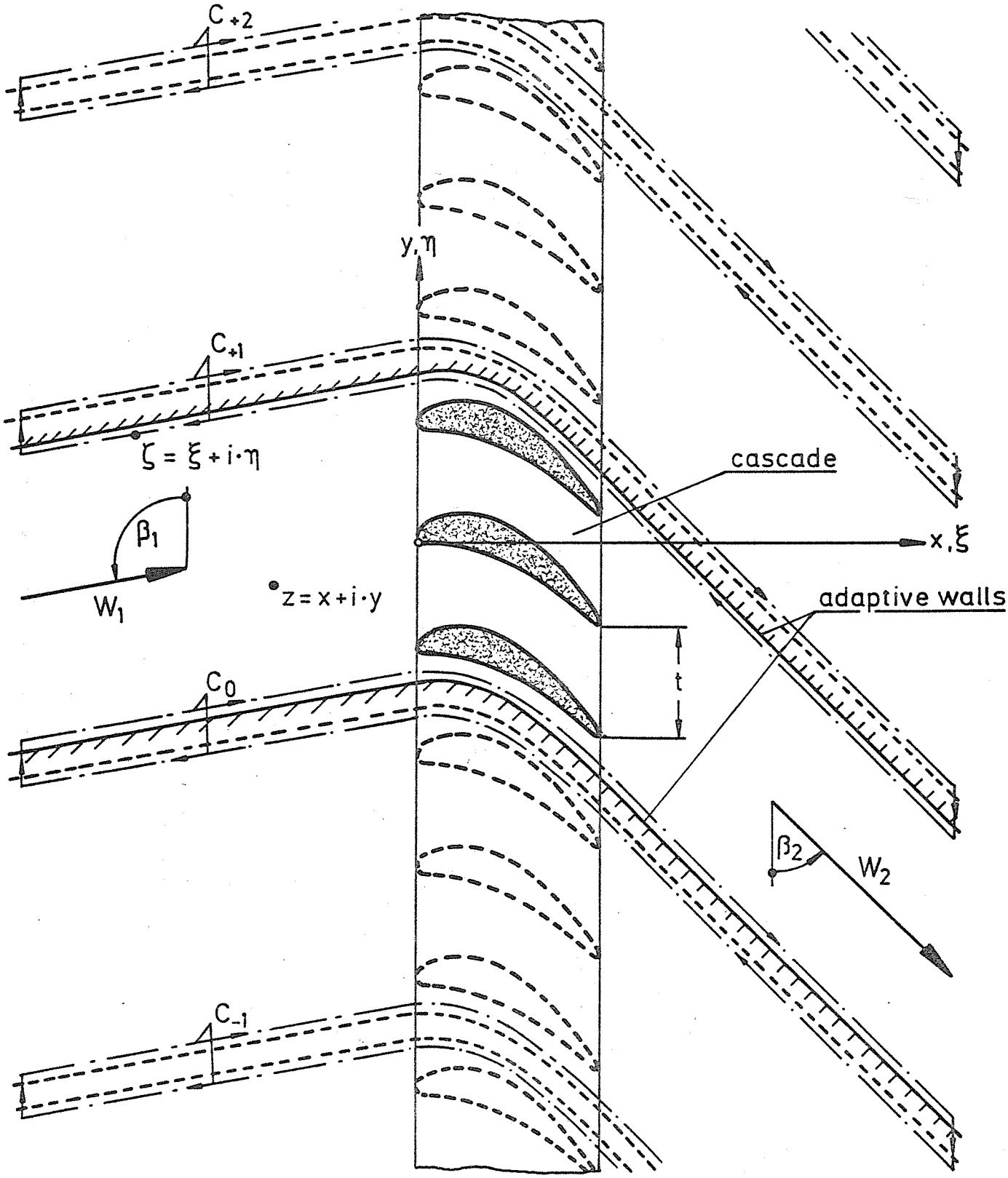

Fig. 2: For the calculation of wall interferences in a cascade test-section

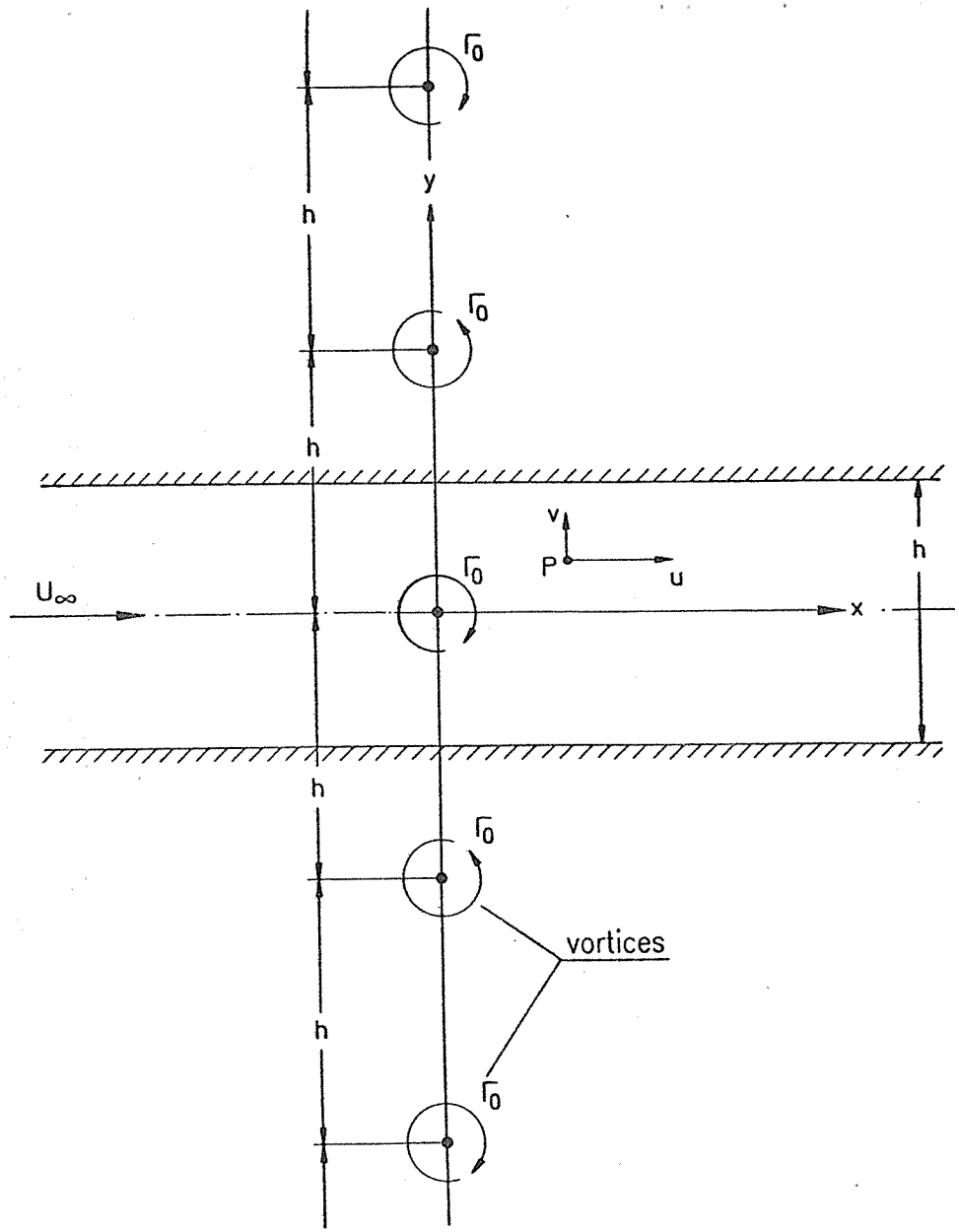

Fig. 3: Superposition of vortex and uniform flow in a straight channel

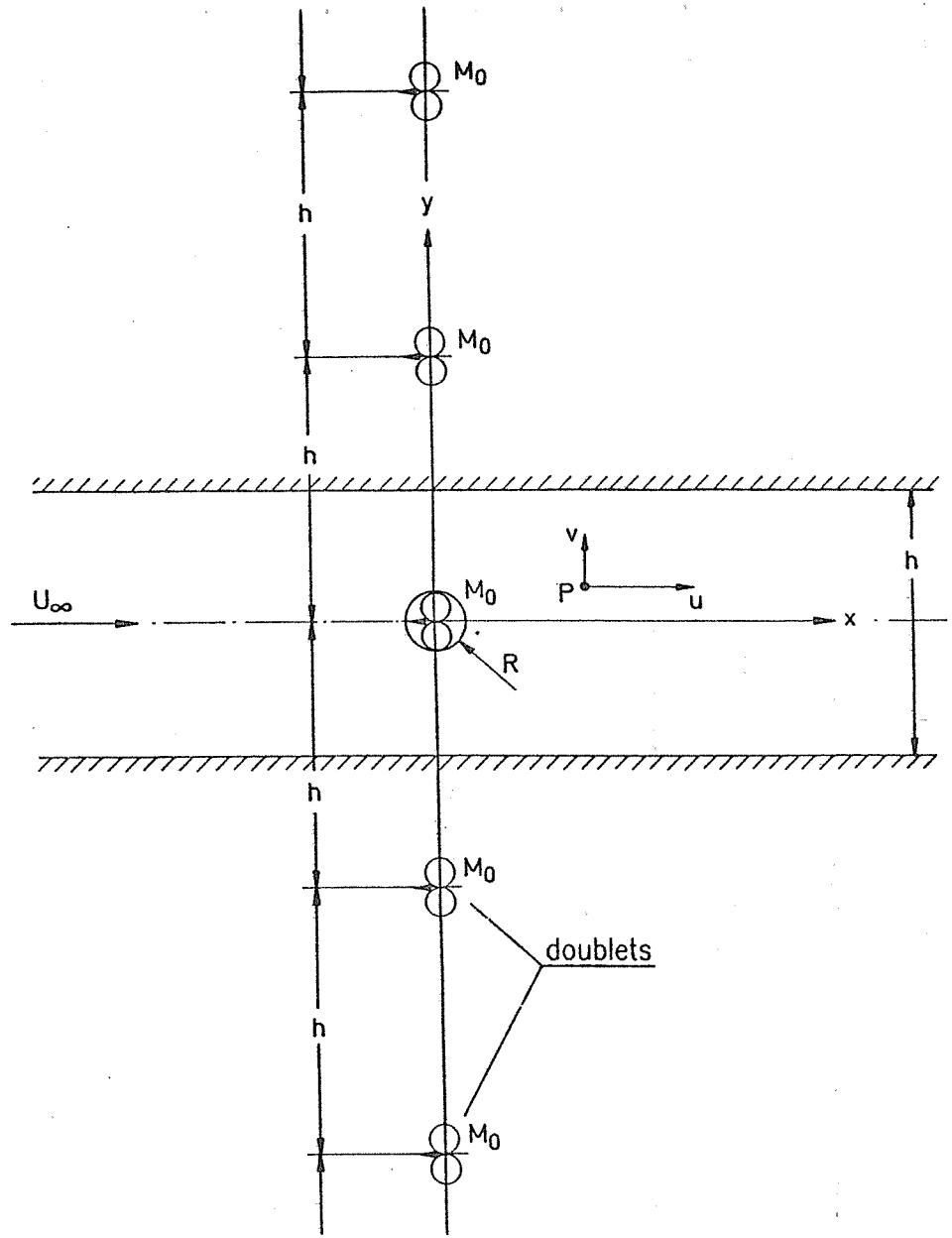

Fig. 4: Superposition of doublet and uniform flow in a straight channel

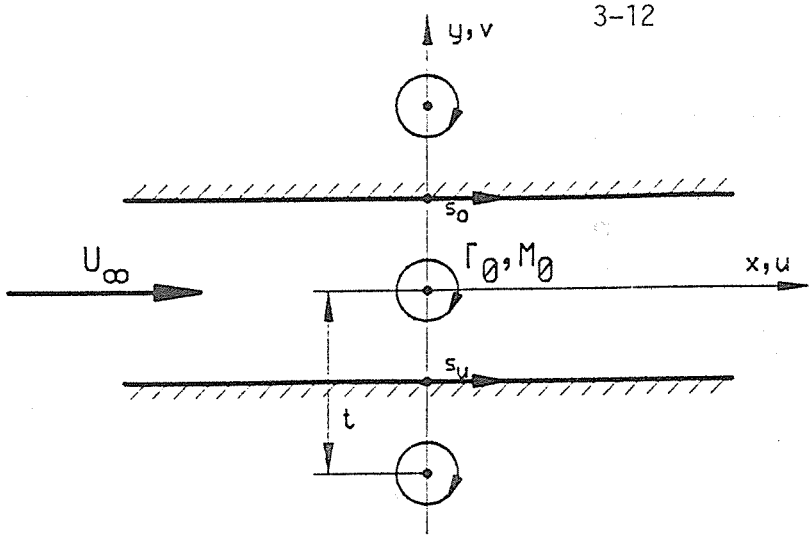

$\Gamma_0 / (2\ t\ U_\infty) = .087$

$M_0 / (2\ \Pi\ U_\infty R^2) = 1.000$

$R / t = .100$

— — — — not adapted

——— adapted

Δ upper contour

∇ lower contour

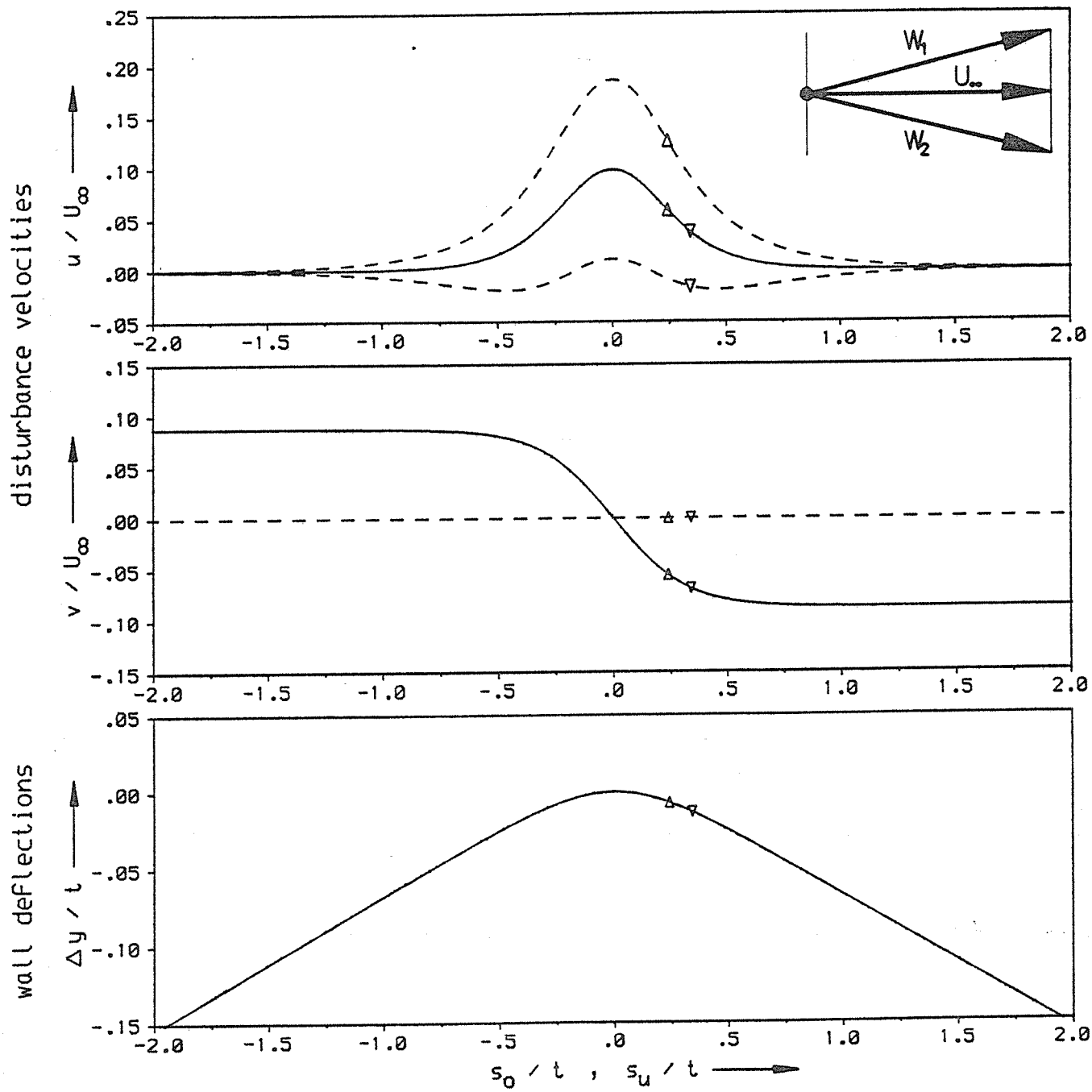

Fig. 5: Disturbance velocities and wall deflections for an unstaggert cascade of rotating cylinders

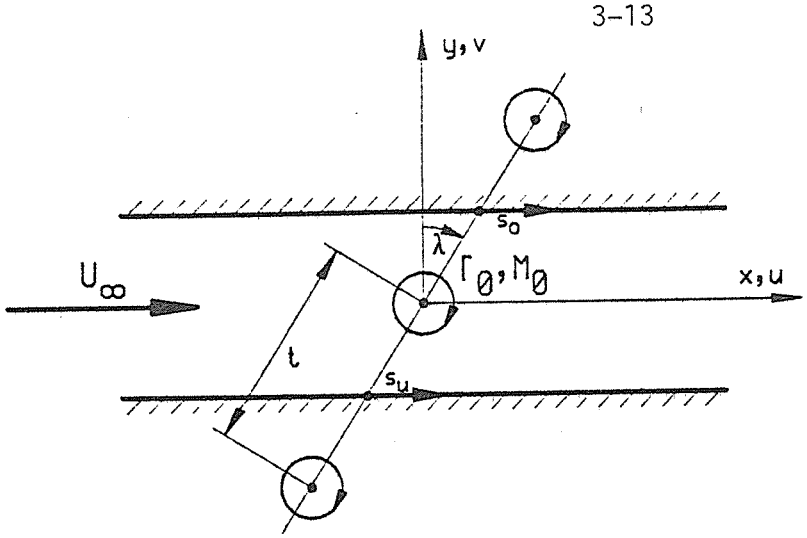

$\lambda = 30.000^{o}$

$\Gamma_0 / (2\ t\ U_\infty) = .087$

$M_0 / (2\ \Pi\ U_\infty R^2) = 1.000$

$R / t = .100$

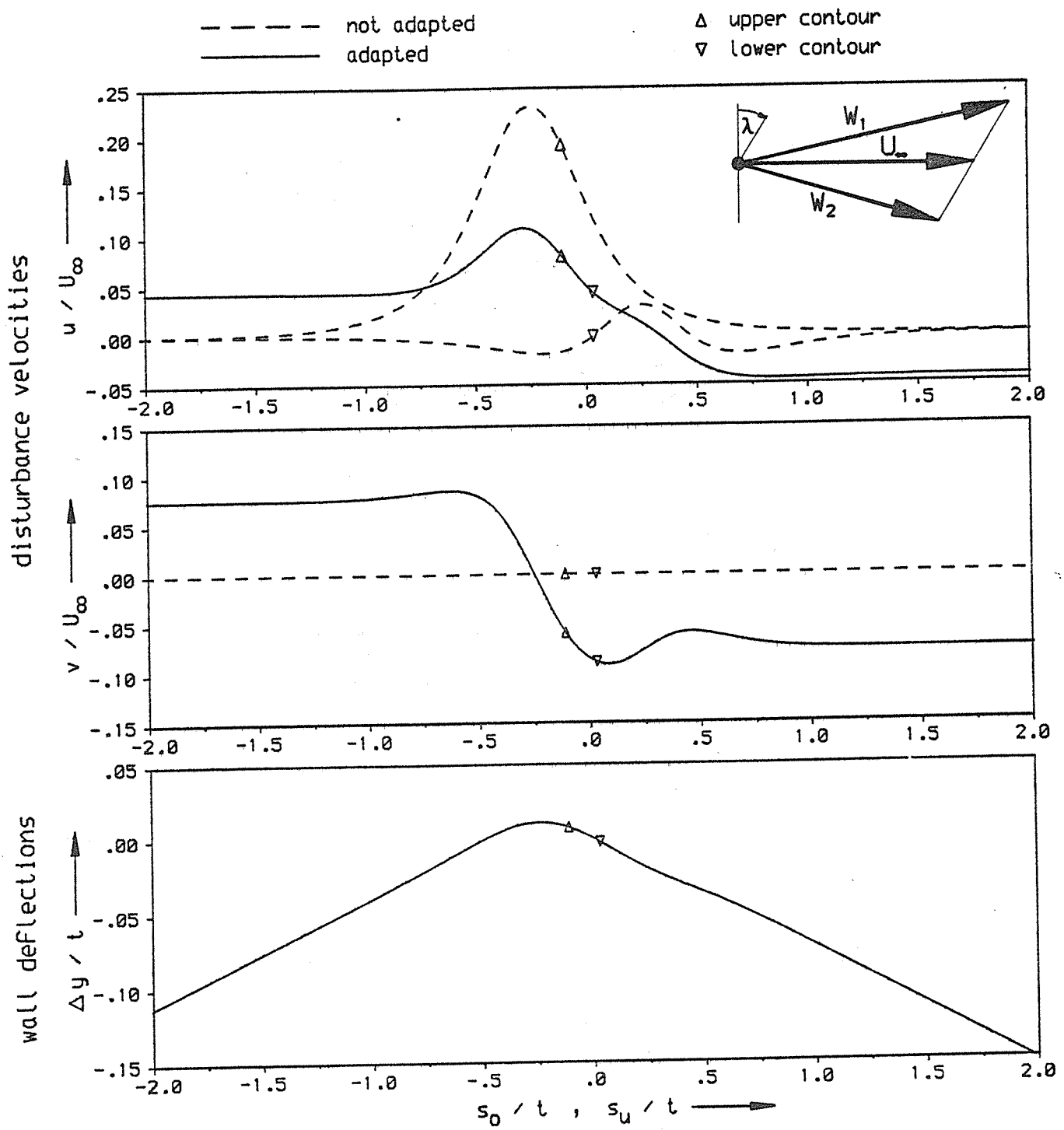

Fig. 6: Disturbance velocities and wall deflections for a staggert cascade of rotating cylinders

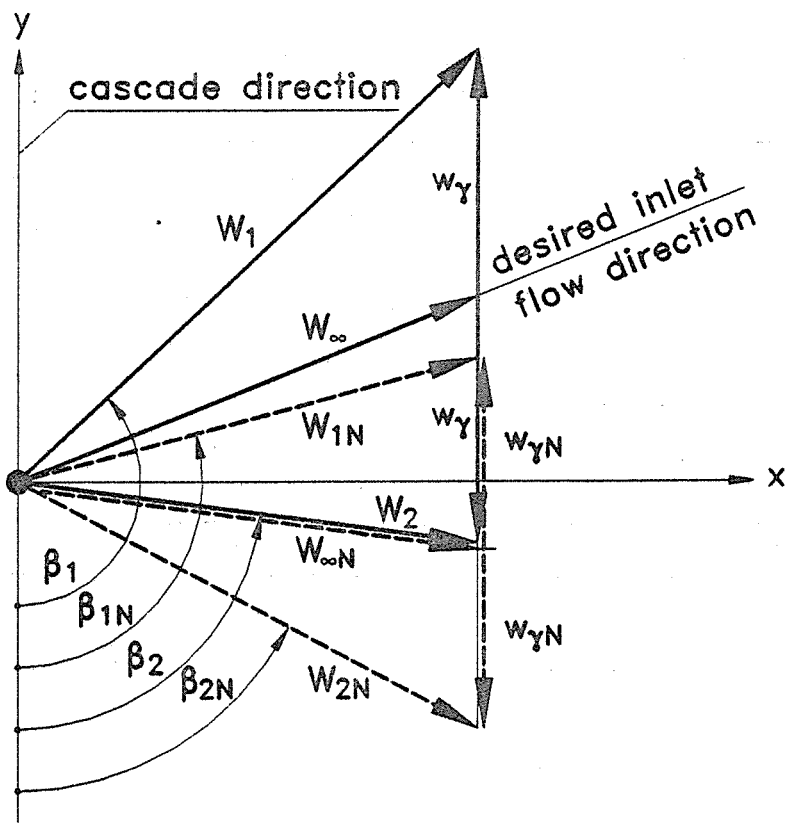

Fig. 7: Setting the free stream velocity vector W_∞ for a desired inlet flow angle (schematic)

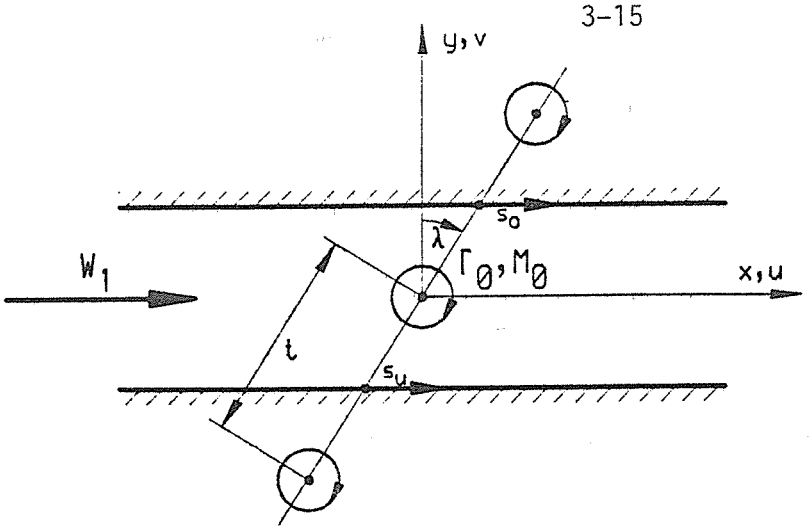

$\lambda = 30.000^{o}$

$\Gamma_0 / (2\ t\ W_1) = .044$

$M_0 / (2\ \Pi\ W_1\ R^2) = 1.000$

$R / t = .100$

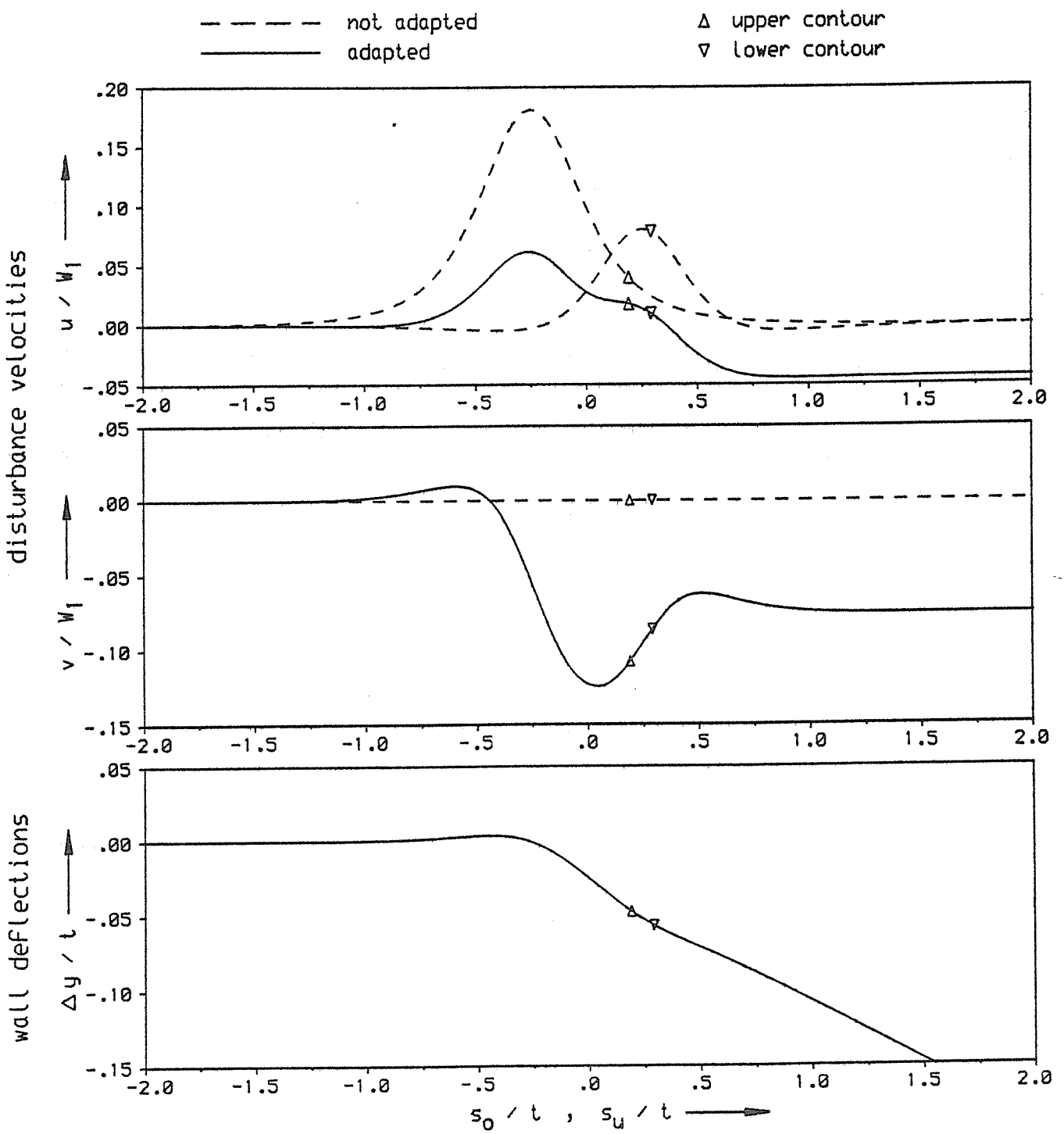

Fig. 8: Disturbance velocities and wall deflections for a staggert cascade of rotating cylinders ($\beta_1 = 90° + \lambda = 120°$)

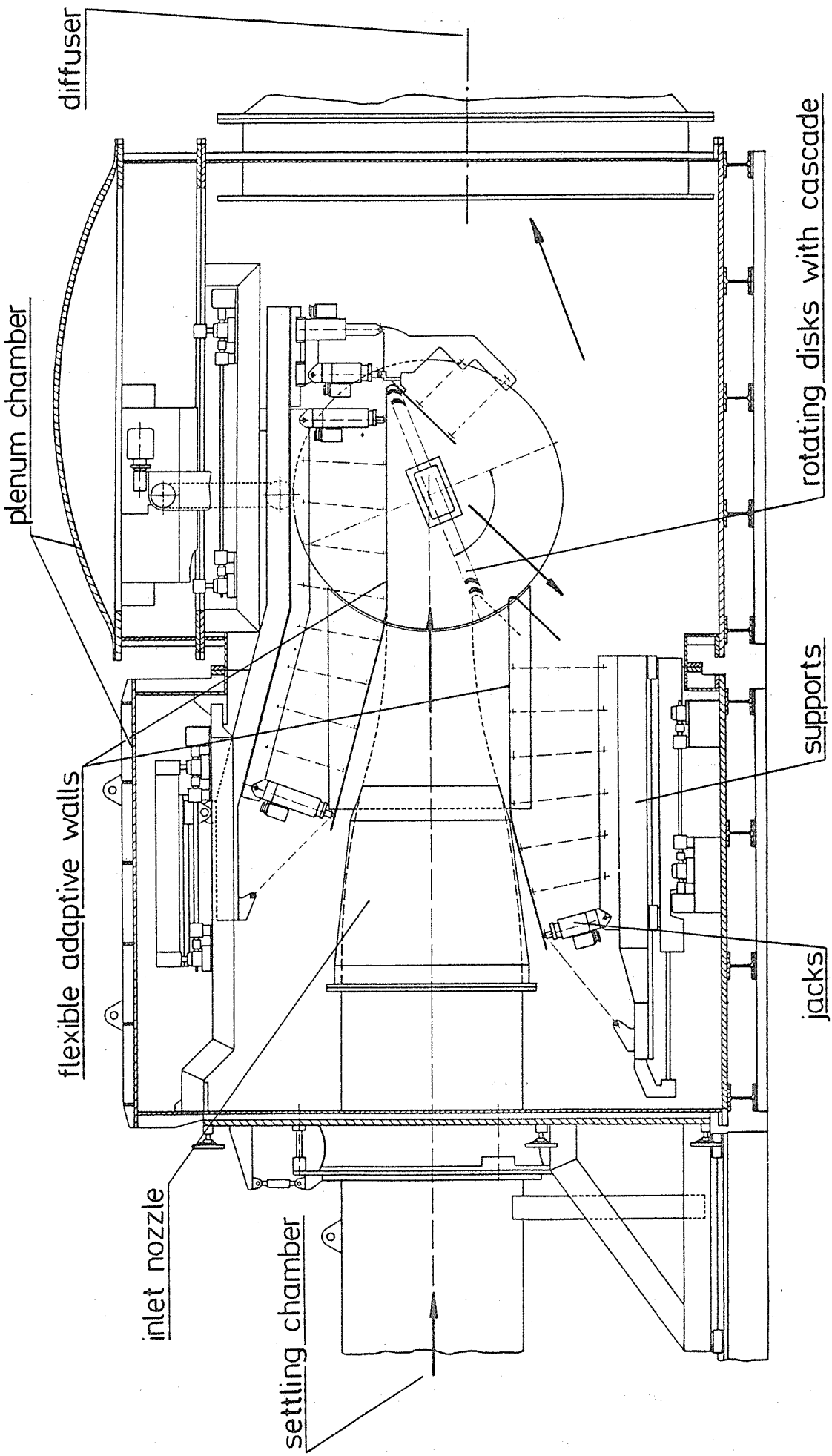

Fig. 9: An adaptive walled cascade test-section in the wind tunnel for rectilinear cascades (EGG) of the DLR